(3430 cm^{-1}) like bands in hydroxyl stretching mode region in FTIR indicates that the tremolites have undergone some structural modifications. From the anomalies in the hyperfine structure of EPR spectra, the field distortion parameter D was estimated to be $(8.5 \pm 2.0) \times 10^{-3}$ cm^{-1} and $(9.2 \pm 2.0) \times 10^{-3}$ cm^{-1}, respectively. The isotropic behaviour of Fe resonance lines in both the samples indicates that it is located on an equivalent site of Mg in this tremolite. All these observations indicate that the tremolites have undergone some structural modifications plausibly due to the metamorphic events associated with the regions.

1. Hawthorne, F. C., *Rev. Mineral.*, 1981, **9**.
2. Jenkins, D. M. and Clare, A. K., *Am. Mineral.*, 1990, **75**, 358–366.
3. Deer, W. A., Howie, R. A. and Zussman, J., *An Introduction to the Rock Forming Minerals*, Longman Scientific & Technical Publ, ELBS edition, London, 1992.
4. Abragam, A. and Bleaney, B., *Electron Paramagnetic Resonance of Transition Ions*, Clarendon Press, Oxford, 1970.
5. Hawthorne, F. C., Ventura, G. D. and Robert, J., *Am. Mineral.*, 1996, **81**, 782–784.
6. Skogby, H. and Rossman, G. R., *Phys. Chem. Mineral.*, 1991, **18**, 64–68.
7. Barabanov, A. V., Zorina, M. A. and Sobolev, V. K., *Mater. Mineral. Kolsk. Poluostrova*, 1974, **10**, 165–175.
8. Blaha, J. J. and Rosasco, G. J., *Anal. Chem.*, 1978, **50**, 892–896.
9. Low, W., *Adv. Electron. Electron Phys.*, 1968, **24**, 51–108.
10. Golding, R. M., Newan, R. H., Rae, A. D. and Tennant, W. C., *J. Chem. Phys.*, 1972, **57**, 1912–1918.
11. Manoogian, A., *Can. J. Phys.*, 1968, **46**, 129–133.
12. McGravin, D. G., Palmer, R. A., Tennant, W. C. and Devine, S. D., *Phys. Chem. Mineral.*, 1982, **8**, 200–205.
13. Naha, K., Mukhopadhyay, D. K. and Mohanty, R., in *Precambrian of the Aravali Mountain* (ed. Roy, A. B.), Geological Society of India, Bangalore, 1988, pp. 207–245.
14. Naha, K., Mukhopadhyay, D. K., Mohanty, R., Mitra, S. K. and Biswal, T. K., *Tectonophysics*, 1984, **105**, 193–206.
15. Spear, F. S., *Metamorphic Phase Equilibria and Pressure Temperature Time Paths*, Mineralogical Society of America, Washington, 1993.
16. Sharma, S. K., Simons, B. and Yoder, Jr. H. S., *Am. Mineral.*, 1983, **68**, 1113–1125.
17. Carmichael, R. S. (ed.), *Handbook of Physical Properties of Rocks*, CRC Press, Florida, 1982, vol II.
18. Skogby, H. and Rossman, G. R., *Am. Mineral.*, 1989, **74**, 1059–1069.
19. Xu, H., Veblen, D. R., Luo, G. and Xue, J., *Am. Mineral.*, 1996, **81**, 1126–1132.
20. Angus, J. G., Raynor, J. B. and Robson, M., *Chem. Geol.*, 1979, **27**, 181–205.
21. Hassib, A., *Phys. Chem. Mineral.*, 1980, **6**, 31–36.

ACKNOWLEDGEMENTS. We thank Dr H. K. Gupta, Director, NGRI for his encouragement and for permission to publish the paper. We also thank the anonymous reviewers for their stimulating comments.

Received 22 February 1999; revised accepted 5 January 2000

Seismogenesis and deformation in the Deccan Volcanic province, Peninsular India

M. Radha Krishna*[,#] and T. M. Mahadevan[†]

*Department of Marine Geology & Geophysics, Fine Arts Avenue, Cochin University of Science & Technology, Cochin 682 016, India.
[†]'Sree Bagh', Ammankoil Road, Cochin 682 035, India

Fault stability margin (SM) due to Deccan Trap overburden estimated for limiting boundary conditions and pore pressures that are not lithostatic is highest along the western pericontinental belt of active rifts (BARS) ($h = 1.5$ km, SM ~ 146 bars). Despite maximum strengthening of weak faults, the frequency of earthquakes is the highest in the BARS. Seismogenesis in the BARS is, therefore, attributed to augmentation of compressive stresses, though erosion and isostatic uplift may play a subordinate role in the southern part. The SM for pore pressures that totally cancel the normal stress is zero but it is suggested that such conditions may be rare where the hypocentres are shallow and the weak faults are possibly open to the surface.

The strain rates for events of $M \geq 4.0$ and/or $I \geq 5$ in the time span 1750–1997 AD (247 years) are the highest for the Kutch seismic domain, being 3.5×10^{-8}/yr. They are similar for the BARS and SONATA belt being $1.2–1.5 \times 10^{-11}$/yr, and are lower by an order of magnitude ($1.7–4.2 \times 10^{-11}$/yr) in the Godavari and Saurashtra domains which have a more closely comparable continental crustal structure. The moment rate tensors estimated for BARS indicate the dominance of N-S compressional stresses. In view of preferred N-S orientation of BARS, we tend to believe that ridge push forces along the mid-Indian Ocean ridges may have a dominant contribution to the stress field of this region matching the Himalayan back thrust. The difference in moment release pattern between the BARS and the SONATA belt is probably due to the contrasting deep continental structure of these regions. The uncertainties in estimation of seismic moments, particularly for historical events, and other assumptions render the above conclusions tentative. However, differences of one or two orders of magnitude in strain rates and concordance of observations with geological and stress field measurements enhance their credibility.

THIS paper addresses three aspects of the seismicity of the Deccan Volcanic Province (DVP): (a) The effect of Deccan basalt cover on strengthening weak faults in the Precambrian basement; (b) The scalar moment release and strain rates in the different crustal provinces within the DVP, and comparison of the same with one of the Gondwana grabens (mid-Phanerozoic) outside the DVP; (c) The moment rate tensor and the diagonalized velocity tensor in part of the DVP most frequented by earthquakes, namely the western pericontinental belt of active rift systems (BARS), for which relevant data are available.

[#]e-mail: mr_radhakrishna@hotmail.com

The DVP has been classified into a number of crustal provinces based on deep continental structure and tectonic and other geological features[1]. These include (i) the western pericontinental belt of active rifts (BARS), (ii) Saurashtra

Continental Block (SCB), (iii) the Narmada–Tapti–Son belt of continental rifts (often referred to as the SONATA belt), (iv) south-eastern platformal block, south of the SONATA belt and east of the BARS, and (v) the north-eastern platformal block, north of the SONATA belt and east of the BARS (Figure 1). The distinct features of these crustal provinces are discussed by Mahadevan[1] and Mahadevan and Subbarao[2]. Some of the major features are summarized in Table 1.

The SONATA belt merges with the BARS west of long 74°E. East of this longitude, it has a distinctive crustal structure as indicated in Table 1. Much confusion seems to have entered into literature by attributing to the whole SONATA belt, the features such as, for example, asthenospheric upwelling, prominent and well established only in the western part[2].

Seismic events of intensity 5 and/or magnitude 4 and above experienced in each of the crustal provinces compiled from various sources[3–8] are listed in Table 2. Figure 2 shows some of the major events listed in Table 2 along with available source mechanisms in the DVP region. The eight focal mechanisms shown in the figure include 1967 Koyna (ref. 3), 1969 Mt. Abu (ref. 3), 1970 Broach (ref. 9), 1973 Bhatsa (ref. 5), 1980 Koyna (ref. 5), 1986 Valsad (ref. 5), 1993 Latur (ref. 6) and 1997 Jabalpur (ref. 8). Though Kutch may be considered as part of the BARS, because of very high magnitudes of the earthquakes in this region and the possibility that close proximity to Baluchistan arc front might influence the Kutch seismicity, the events in the Kutch region are treated separately.

Johnston[10] analysed the strengthening influence of thick ice sheets of Greenland and Antarctica on weak faults underlying them in a compressive environment. He quantified the stabilizing influence in terms of the fault stability margin (SM) in the Coloumb–Mohr fault failure stress representation, for a spectrum of conditions with limiting lateral and lithostatic constraints and different pore pressures. The DVP is characterized by thick but variable cover of Deccan Volcanic flows, which like the ice sheets may strengthen weak faults in the basement. The SM over an area of the DVP falling

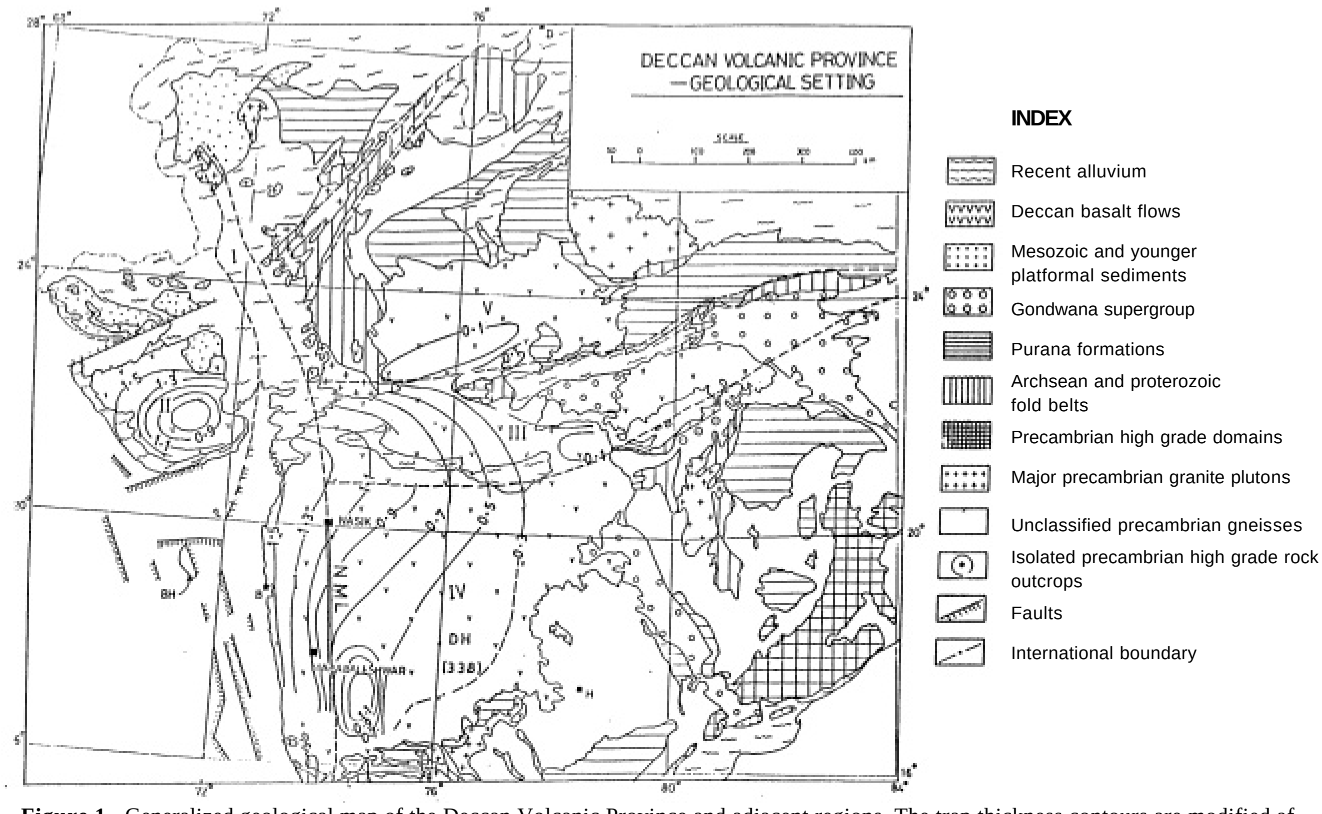

Figure 1. Generalized geological map of the Deccan Volcanic Province and adjacent regions. The trap thickness contours are modified after Kaila[12]. B, Bombay; BH, Bombay High; DH, Drill Hole; H, Hyderabad, NML, Nasik–Mahabaleswar Line of volcanoes; 338, Depth in meters to granitic basement below traps. I, BARS; II, SCB; III, SONATA; IV, SEPB; V, NEPB.

Table 1. Some major geophysical characteristics of different crustal domains in the Deccan Volcanic Province. Data summarized from Mahadevan[1]

Parameter	BARS	SONATA	SCB	SEPB	NEPB
Major tectonic setting	Active rifting	Horst–graben tectonism	Reactivated continental platform	Continental platform (passive)	Continental platform (passive)
Deccan Trap	1–1.5	<1.0	1–0	<1.0	<0.6
Crustal thickness (in km)	18–30 (S)	38–45 (S)	38–42 (S)	38 (S)	>40 (G)
Depth to conrad (in km)	6–18	0–18	12–16	~20	n.d.
Lithosphere thickness	70 (?) (E) (S)	100 (?) (S)	n.d.	>250 km (T) (P)	>250 km (P)
Magnetization from Magsat data	(+) and (–)	(+)	(–)	(+)	(+)
Regional gravity (mgal)					
Bouger	+50 to –110	–10 to –30	–20 to +70	–10 to –100	–10 to –80
Isostatic (Airy)	+50 to –70	+40 to –40	+40 to –30	–10 to –60	+10 to –30
Heat flow (in mWm^{-2})	≤80	≤60	high	~41	n.d.

(G), Estimated from gravity data; (S), Estimated from seismic data; (E), Electrical conductivity, n.d., no data; (T), Seismic tomography, (P), Petrological data.

between lat. 22°N and 16°N and long. 73°E and 78°E for which data on trap thicknesses are better known, are evaluated for the boundary conditions followed by Johnston.

In general terms, the trap cover is thickest over the Western Ghats, especially along the Kalsubai–Mahabaleswar axis and is estimated to be of the order of 1.5 km, reaching a maximum of 2 km locally. The trap cover thins down eastwards and within some 500–600 km the Precambrian basement is exposed. In the low Konkan plains, west of the erosional scarps of the Western Ghats, the trap thickness is < 1 km, the upper part of the trap having been removed by erosion[11]. However, due to the westerly dip the trap thickness increases to 1.2 km along the coastal tract. A generalized contour map of the trap thicknesses has been generated by Kaila[12], from DSS profiles across several sections of the DVP and is used here with some modifications. Recent drilling in Killari (Latur) (DH in Figure 1) has revealed a thickness of 338 m of traps[13] and the trap thickness contours of Kaila have been extended to fit this thickness (Figure 1).

In evaluating SM, it is noteworthy that the crust below the DVP is under compressional stress from plate boundary forces[14]. It is assumed that several trap basement faults are weak and at failure threshold. A focal depth of 5 km, average crustal density of 2.7 g/cc, trap density of 2.6 g/cc providing for the low density of vesicular trap flows and friction coefficient of 0.4 are assumed. SM values have been calculated for trap thicknesses of 1.5, 1.0, 0.5 and 0.3 km for the different boundary conditions of lateral and lithostatic constraints and for pore pressures varying from hydrostatic pressure to those equal to trap overburden[15]. Results are presented in Table 3. It may be seen from the table that the SM values range from 146 bars to 4 bars, except when under lithostatic constraint pore pressures cancel the effect of the trap overburden (case V). The features are presented in the Mohr–Coulomb representation in Figure 3.

Following the concept of Kostrov[16], if all the strain in a volume V is seismic, the average strain rate tensor is related to the sum of seismic moment tensors of all earthquakes within it as:

$$\dot{\varepsilon}_{ij} = \frac{1}{2\mu VT}\sum M_{ij}^{n}, \tag{1}$$

where μ is shear modulus of 3.5×10^{11} dyn cm^{-2}, T is the time period of observation and $\sum M_{ij}^{n}$ is the sum of moment tensors of n earthquakes. Since the seismic moment tensor is a combination of scalar moment (M_0) and information derived from the focal mechanism data, in regions where focal mechanism solutions are not available, the same concept could be extended to compute simple strain rate from the cumulative scalar seismic moment release. Brune[17] observed that such estimates obtained from the cumulative moment release would represent the true deformation pattern if the time interval of observation is sufficiently long to include large earthquakes. In the present study, we utilized the earthquakes that occurred during 1750–1997 (Table 2) to calculate the cumulative moment release and strain rates in different crustal provinces of the DVP. Except for a few events (e.g. Latur and Jabalpur) having seismic moments, for the rest of the events either intensities or magnitudes are only available. For all the events with intensities, their equivalent magnitudes given by Rao

Table 2. Catalogue of major earthquakes (M > 4.0 and/or I.5) in the DVP and the Godavari–Gondwana rift

	Latitude	Longitude	Magnitude/

Sl. No.	Date	Locality	(°N)	(°E)	Intensity	Reference
BARS 1. Cambay–Bombay–Ratnagiri zone						
1	09–12–1751	Salsette Region	19.1	73.2	VI	3
2	05–01–1752	Salsette Region	19.1	73.3	V	4
3	05–02–1752	Lohagarh	18.7	73.4	V	3
4	*–08–1764	Mahabaleswar	17.9	73.7	VII	3
5	29–05–1792	Jangira	18.5	73.0	V	3
6	13–08–1821	Kaira–Damaun–Ahmedabad	22.7	72.7	V	3
7	20–03–1826	Moze Morvade	16.1	73.6	VI	3
8	10–11–1840	Ahmedabad	23.0	72.7	V	4
9	09–10–1842	Baroda	22.3	73.2	V	3
10	25–12–1856	Dahanu	20.0	73.0	VII	3
11	29–04–1864	Ahmedabad–Surat	22.3	72.8	VII	3
12	15–12–1882	Mt. Abu	24.9	72.7	VI	4
13	*–*–1951	Jaigram	17.3	73.2	V	4
14	01–09–1962	North Gujarat	24.0	73.0	5.0	3
15	04–06–1965	Ratnagiri	17.0	73.4	5.4	4
16	25–04–1967	Mahad	18.2	73.4	5.6	4
17	19–05–1967	Ratnagiri	17.0	73.5	V	3
18	20–06–1967	Alibagh	18.7	73.0	V	3
19	13–09–1967 to 1973	Koyna			5.6 to 7.0	3, 4
20	07–03–1969	Sangameshwar	17.2	73.6	4.7	4
21	24–10–1969	Mt. Abu	24.8	72.4	5.3	4
22	23–03–1970	Broach	21.7	73.0	5.4	4
23	30–08–1970	Broach	21.6	72.7	4.1	4
24	17–02–1974	Near West Coast	17.5	73.1	5.0	4
25	14–03–1976	Koyna Region	17.3	73.7	4.8	7
26	19–09–1977	Koyna Region	17.3	73.64	5.0	5
27	02–09–1980	Koyna Region	17.27	73.71	4.7	5
28	20–09–1980	Koyna Region	17.25	73.70	4.9	5
29	20–09–1980	Koyna Region	17.26	73.64	5.2	7
30	25–09–1980	Koyna Region	17.4	74.20	4.9	7
31	04–10–1980	Koyna Region	17.2	73.82	4.8	7
32	14–09–1983	Bhatsa	19.57	73.4	4.9	5
33	25–09–1983	–	17.29	73.97	4.6	7
34	14–11–1984	–	17.28	73.96	4.5	7
35	27–04–1986	Valsad	20.56	73.34	4.6	5
36	15–11–1986	Aravalli	24.9	74.2	4.8	5
BARS 2. Kutch Zone						
37	16–06–1819	Kutch	23.6	69.6	XI	3
38	20–07–1828	Bhuj	23.2	69.9	V	4
39	*–*–1844	Lakhpat	23.8	68.9	V	4
40	19–04–1845	Lakhpat	23.8	68.9	VII	4
41	19–06–1845	Delta of Indus	23.8	68.9	VIII	4
42	14–01–1903	Kutch	24.0	70.0	6.0	4
43	26–10–1921	Jerruck	25.0	68.0	5.5	4
44	14–06–1950	Bhuj	24.0	71.2	4.7	4
45	21–07–1956	Anjar	23.0	70.0	7.0	4
46	13–07–1963	Thar Parkar	24.9	70.3	5.6	4
47	26–03–1965	North of Kutch	24.4	70.0	5.3	4
48	27–05–1966	South of Hyderabad	24.5	68.7	5.1	4
49	23–03–1969	South of Hyderabad	24.4	68.7	4.4	4
50	13–02–1970	South of Hyderabad	24.6	68.6	5.2	4
51	31–01–1982	Pak Border	24.1	69.6	4.8	7
52	18–07–1982		23.4	70.6	4.8	7
53	07–04–1985	Indo–Pak Border	24.3	69.9	5.0	7
54	10–10–1986		24.8	68.9	4.7	7
55	10–12–1989		24.8	70.8	4.6	7
56	10–12–1989		24.6	70.9	4.7	7

Contd.

Table 2. (*Contiued*)

Sl. No.	Date	Locality	Latitude (°N)	Longitude (°E)	Magnitude/ Intensity	Reference

57	20–01–1991		23.0	69.5	4.9	7
58	20–01–1991		23.3	69.7	4.9	7
59	10–09–1991		24.1	68.6	4.7	7
60	10–09–1991		24.2	68.8	4.8	7
61	10–09–1991		24.1	38.6	4.7	7
62	10–09–1991		24.1	68.8	4.8	7
Saurashtra Continental Block (SCB)						
63	24–01–1919	Bhavnagar Para	22.0	72.0	VII	4
64	13–03–1922	Patoi–Jhalawad–Rajkot	22.0	71.0	V	4
65	June 1938	Paliyad	22.3	71.6	VI	4
66	14–07–1938	Paliyad	22.4	71.8	VI	4
67	23–07–1938	Paliyad	22.4	71.8	VII	4
68	31–10–1940	North–West Kathiawar	22.5	70.4	VI	4
69	24–08–1993	Off Saurashtra	20.6	71.3	5.0	4
SONATA Belt						
70	27–05–1846	Narmada	23.0	80.0	VI	3
71	08–11–1863	Nimah–Burwani	21.8	75.3	VII	4
72	02–06–1927	Son Valley	23.5	74.3	6.5	4
73	14–03–1938	Satpura	21.5	75.7	6.3	4
74	25–08–1957	Balaghat	22.0	80.0	5.5	3
75	06–01–1967	Raipur	22.0	74.3	4.3	4
76	14–11–1968	Betul	21.8	78.0	4.2	4
77	26–03–1969	Itarsi	22.3	77.8	4.2	4
78	20–10–1974	Taloda	21.7	74.2	4.6	4
79	13–08–1975	Betul	21.8	77.7	4.1	4
80	25–09–1975	West of Dhulia	20.8	74.2	4.2	4
81	18–04–1987		25.52	79.24	4.8	–
82	22–05–1997	Jabalpur	23.08	80.06	6.0	8
South–Eastern Platformal Block						
83	29–09–1993		18.3	76.8	4.8	–
84	30–09–1993	Latur/Killari	18.0	76.5	6.4	6
North–Eastern Platformal Block						
85	21–12–1926	Lukwasa	25.0	77.5	5.5	4
86	10–04–1929	Lukwasa	25.0	77.5	5.5	4
87	25–06–1930		25.0	77.5	5.5	4
88	28–06–1988		24.9	75.3	4.9	–
Godavari–Gondwana Rift						
89	27–07–1968	Bhadrachalam	17.6	80.8	4.5	7
90	29–07–1968	Bhadrachalam	17.6	80.8	4.5	7
91	13–04–1969	Bhadrachalam	17.9	80.6	5.7	7
92	15–04–1969	Bhadrachalam	18.0	80.7	4.6	7
93	30–04–1969	Bhadrachalam	17.9	80.6	4.5	7
94	18–04–1987	Bhadrachalam	19.1	78.5	4.6	7

and Rao[4] calculated using Gutenberg–Richter relation were considered. The magnitude–moment relations (both Mb–Mo and Ms–Mo) given by Johnston[18] and Mb–ML relations by Veneziano[19] for global SCR earthquake data set were utilized for converting the magnitudes to moments. It is relevant to state here that Brune[17] and Jackson and relevant to state here that Brune[17] and Jackson and McKenzie[20] observed that the procedure for converting magnitude to moment estimation would bring in uncertainties in cumulative moment release by a factor of 5.

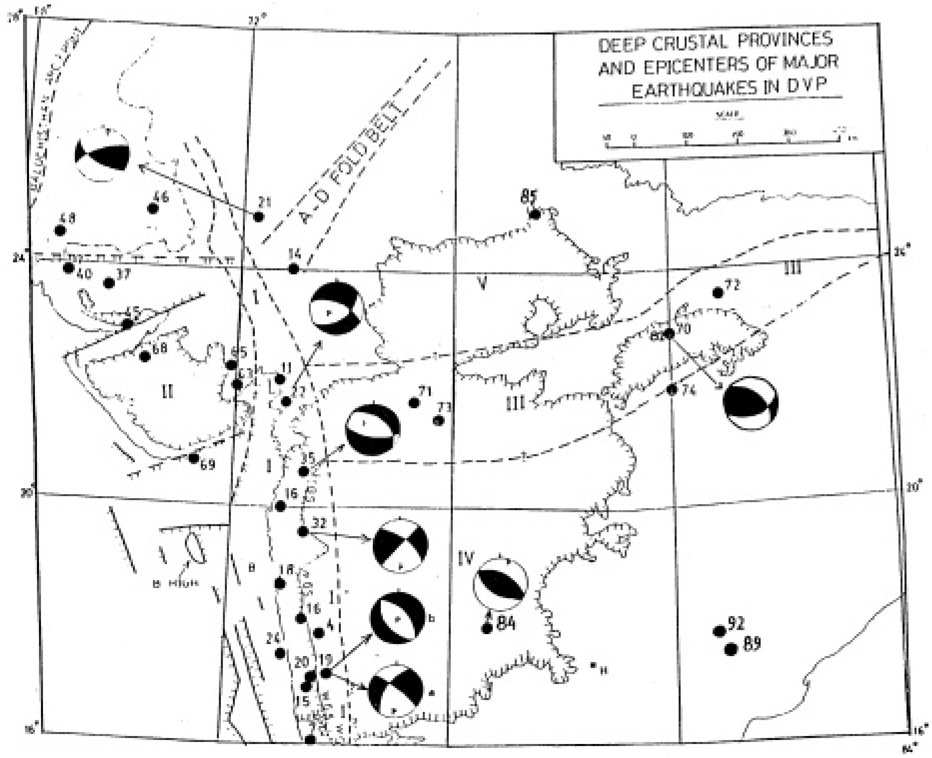

Figure 2. Seismotectonic map of the DVP showing the crustal domains as in Table 1 and major earthquakes listed in Table 2 along with focal mechanism solutions for those available. AD, Aravalli–Delhi Fold Belt; B, Bombay; WGS, Western Ghat Scarp.

Table 3. Stability margin on faults due to different thicknesses of Deccan Trap cover and different boundary conditions

Trap thickness (km)	SM (bar)			
	Case II	Case III	Case IV	Case V
1.5	146.0	65.0	4.0	0.0
1.0	112.0	58.0	17.0	0.0
0.5	78.0	51.0	31.0	0.0
0.3	64.0	49.0	36.0	0.0

Case II, Trap present, lateral constraint, pore pressure P is hydrostatic, $\Delta P = 0$; Case III, Trap present, lithostatic, pore pressure is hydrostatic, $\Delta P = 0$; Case IV, Trap present, lateral constraint, enhanced pore pressure, $\Delta P = +$ ©$_{t}gh$; Case V, Trap present, lithostatic, enhanced pore pressure, $\Delta P = +$ ©$_{t}gh$ (Case I refers to pre-trap crust when SM = 0).

A thickness of 15 km was used for estimating strain rates. The results are given in Table 4. As already stated, the Kutch region has been treated separately in view of the very large magnitude earthquakes in that region and possibilities of that region being distinctive from the rest of the BARS. It can be seen from the table that the differences in strain rates for different provinces are significant even within the probable uncertainties in their estimates referred to above. The main conclusions that emerge from Table 4 are: (a) The Kutch region has the maximum scalar moment release and the highest strain rate, a couple of orders higher than the rest. (b) The BARS, despite the markedly large number of events in it (~70), has still a moment release similar to the SONATA belt. This may imply that the SONATA belt is building up stresses to much higher levels and over longer periods of time. In contrast, stresses are being released in the BARS frequently from relatively shallow depths by fault failure. Though most of the listed events from Koyna region in the BARS are attributed to reservoir-induced seismicity[21,22] the widespread occurrence of earthquakes throughout the BARS points towards the dominant role of tectonic activity, which may, however, be complimented locally (as in Koyna) by the after-effects of reservoir loading. (c) The similarity in the strain rates of the Saurashtra and Godavari belts is consistent with the comparable deep continental structure in the two belts (Table 1).

Available source mechanisms in the BARS, namely those of 1967 Koyna, 1970 Broach, 1986 Valsad, 1983 Bhatsa and 1980 Koyna have been used to calculate the moment rate tensors based on the formulations of Jackson and McKenzie[20]. The strike, dip and slip information inferred from the focal mechanisms were used to obtain individual components of the tensor following Aki and Richards[23]. The individual moment tensor components would be severely affected by errors in the focal

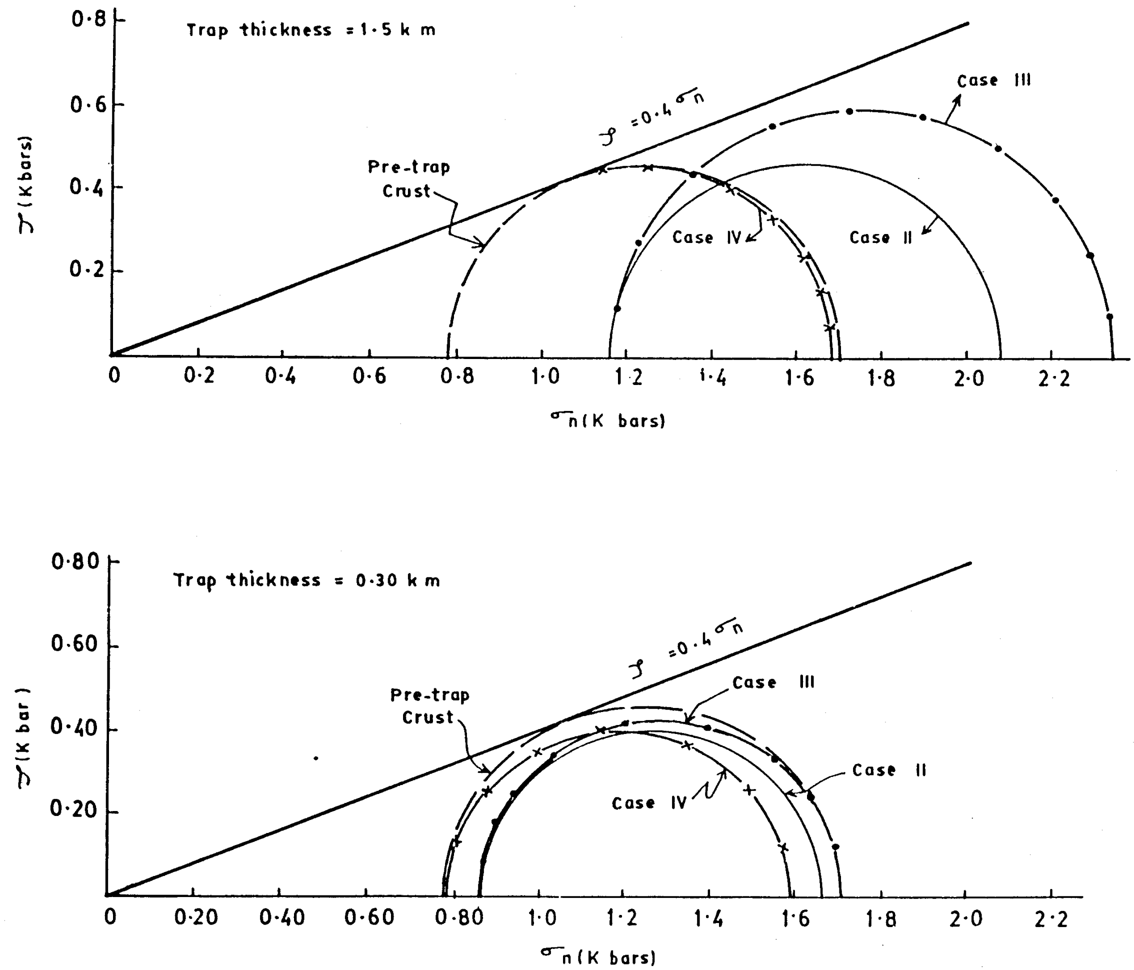

Figure 3. Diagrammatic representation of Mohr–Coulomb criteria for fault failure for two extreme trap thickness values (1.5 km and 0.3 km) and various boundary conditions mentioned in Table 3.

mechanisms, whose accuracies are not certain, as they have been derived from the first motion data. Further, moment tensor computations are based on several assumptions. It is assumed that the strain release in a given volume is completely seismic, the volume of the seismic zone is well-defined and the catalogue of earthquake is complete for all magnitudes for the period of computation. However, within these limitations, the results do provide a first-order picture of the deformation pattern. The north (x_1), east (x_2) and down (x_3) reference system was used in the calculation of moment tensors. Since the BARS orient along N-S, no rotation in the zone reference system is required. The velocity tensor calculated from the moment tensor elements have been diagonalized to obtain the principal components of velocity tensor. Table 4 reveals that U_{11} is the dominant component with the –ve sign indicating compression. The –ve sign in U_{33} indicates crustal thinning, the value being insignificant. In other words, N-S compressive regime seems to be more dominant without significant indication of vertical uplift for the BARS as a whole.

The SM provided by the Deccan Trap cover and the seismological parameters of earthquakes in the BARS and the SONATA belt presented here have a potential to constrain the tectonic milieu in which the earthquakes are generated.

The SM values due to Deccan Trap cover progressively increase from Latur in the SEPB westwards into the BARS as the thickness of the traps increases. Despite such increase in the SM values, the BARS is seismically far more active than the SEPB. The increase in seismicity may be due to any one or all the three factors, namely increase in pore pressure, isostatic uplift and amplification of the compressive stresses. We now examine the possible implications of each of these factors in the DVP, particularly in the BARS and the SONATA belt.

BARS has a predominance of shallow focus earthquakes. It is characterized by numerous hot springs that reflect the openness of the fracture systems, a condition in which pore pressures may not exceed the hydrostatic pressures. However, new blind fractures, if generated,

Table 4. Cumulative moment release and strain rates estimated for various geotectonic regions in and around the DVP for the period 1750–1997. The focal mechanisms available for BARS were utilized to calculate moment tensors in that region (thickness of seismogenic layer assumed to be 15 km and rigidity 3.5×10^{11} dyn cm^{-2}). The –ve values in moment tensors indicate compression and +ve values extension

Region (Length and width in km)	No. of earthquakes	Maximum magnitude	Cumulative moment release $\times 10^{24}$ dyn cm	Strain rate $(yr)^{-1}$
Scalar moment release				
Kutch seismic domain (250, 150)	26	7.8	4233.4	3.5×10^{-8}
BARS (800, 100)	70*	6.0	29.62	1.49×10^{-10}
SONATA belt (900, 200)	12	6.3	57.7	1.2×10^{-10}
Godavari graben (450, 75)	6	5.7	1.52	1.7×10^{-11}
SCB (250, 250)	7	5.5	6.8	4.2×10^{-11}

Moment rate tensors ($\dot{M}$) and deformation velocities (U mm/yr) for BARS

	11	22	33	12	13	23
M	–0.064	0.041	0.015	0.036	–0.034	–0.036
U	–0.061	0.005	0.0003	0.009	–0.001	–0.001

Eigen values for the velocity tensor

U_{11}	U_{22}	U_{33}
–0.062	0.0071	–0.00001

*Also include several Koyna events of $M_s > 5.0$.

may lead to high pore pressures till such fractures too get opened and linked to the surface.

The Deccan Trap region is known as a region undergoing eustatic uplift[24]. Widdowson[25] has advocated that the seismicity of the region may be due to denudational isostasy resulting from large erosion along the Konkan plains and the corresponding sediment loading in the Arabian Sea. On the eastern flank also the erosion is very significant as is evident from a highly dissected fluvial geomorphology of the region. The sediments removed are, however, getting loaded in the far off Bengal Fan. Isostatic response, however, is a slow process, especially when distributed over a period of 65 million years or so (the time that has elapsed after the Deccan volcanism), and it may lead to largely aseismic deformation. The stresses released by denudational isostasy may be dissipated through several processes. Further, any isostatic response has to operate within the compressional field generated by the plate boundary forces and also the fault stability offered by the Deccan Trap loading.

The earthquake source mechanisms in the BARS are thrusts and strike–slip faults. Locally however, as in the 1980 Koyna and the 1986 Valsad events in the southern part of the BARS, normal fault mechanisms have been noted, which may imply distension due to uplift forces or alternatively distension as a local variant of an overall compressive regime. Evaluation of the moment tensors provides significant constraints on the tectonic setting. The smaller uplift component and the dominant N-S component in the moment tensors of the BARS are consistent with the dominance of N-S thrusting in the BARS as a whole. This leads to the conclusion that amplification of stresses is the more dominant factor that renders the BARS seismogenic. The contribution of isostatic uplift to seismic deformation may be minimal and more localized. The main forces acting on the stress field in the BARS could be the Himalayan back thrust and those arising from the kinematics of plate reorganization along the spreading ridges in the Indian Ocean region[26]. To this may be added a possible back thrust from the Baluchistan arc. The preferred N-S orientation of the BARS renders it oblique to all the three forces and it would seem that the forces of compression from the Indian Ocean have to be quite significant to match the Himalayan forces, that can then result in the overall dominance of the compressive field.

The differences in the moment release pattern between the BARS and the SONATA belt referred to earlier may be a reflection of the contrasting deep continental structure below the two regions and the differences in their physical disposition in relation to the Himalaya. Recent findings on the possible neotectonic activity[27,28] and the anomalous crustal structure[29] in the SONATA belt also bring to focus the seismic vulnerability of this belt. Further, trapped layers of high pressure pore fluids in the lower crustal formations and the underplating magmatic rocks of the SONATA belt may enhance such vulnerability by deformation under ‘drained conditions’[2,30].

The Deccan trap cover over the DVP has the potential to strengthen the weak faults in an overall compressive environment to the extent of 146 to 4 bars, except when the pore pressures reach lithostatic levels. Both isostatic uplift and amplification of compressive stresses seem to have the capability to overcome the safety margin induced by the trap cover. But it would seem that in the BARS the latter is the more dominant factor due not only to the Himalayan back thrust, but also due to a significant contribution from the ridge push forces of the Indian Ocean. The scalar moment release and the strain rates of some of the crustal provinces within the DVP differ by an order of magnitude or two. The Kutch region stands out as a distinctive domain of very high strain rate followed by the SONATA belt and the BARS, which have comparable cumulative moment release and strain rates. The Saurashtra crustal block has the least value. Several uncertainties influence the estimation of scalar moment release and strain rates, but, large differences in the values seems to lend credibility to the conclusions drawn.

Between the BARS and the SONATA belt, the latter seems to have greater capability to accumulate energy and release the same in much fewer events, while the former is releasing energy more frequently and from much shallower levels. The isostatic rebound associated with the southern part of the BARS may have only a subordinate role in such release mechanism.

1. Mahadevan, T. M., *Mem. Geol. Soc. India*, 1994, **28**, 237–301.
2. Mahadevan, T. M. and Subbarao, K. V., *Mem. Geol. Soc. India*, 1999, **43**, 453–484.
3. Chandra, U., *Bull. Seismol. Soc. Am.*, 1977, **67**, 1387–1413.
4. Rao, B. R. and Rao, P. S., *Bull. Seismol. Soc. Am.*, 1984, **74**, 2519–2533.
5. Rastogi, B. K., *Curr. Sci.*, 1992, **62**, 101–108.
6. Gupta, H. K., *Mem. Geol. Soc. India*, 1994, **35**, 1–5.
7. Gowd, T. N., Srirama Rao, S. V. and Chary, K. B., *Pure Appl. Geophys.*, 1996, **146**, 503–531.
8. Bhattacharya, S. N., Ghose, A. K., Suresh, G., Baidy, P. R. and Saxena, R. C., *Curr. Sci.*, 1997, **73**, 855–863.
9. Arora, S. K., Nair, G. J. and Varghese, T. G., *Earthqu. Notes*, 1970, **XLI**, 17–26.
10. Johnston, A. C., in *Earthquakes at North Atlantic Passive Margins: Neotectonics and Postglacial Rebound* (eds Gregersen, S. and Basham, P. W.), Kluwer Academic Press, Dordrecht, 1989, pp. 581–599.
11. Widdowson, M. and Cox, K. G., *Earth Planet. Sci. Lett.*, 1996, **137**, 57–69.
12. Kaila, K. L., *Mem. Geol. Soc. India*, 1988, **28**, 239–301.
13. Gupta, H. K. and Dwivedy, K. K., *J. Geol. Soc. India*, 1996, **47**, 129–131.
14. Gowd, T. N., Srirama Rao, S. V. and Gaur, V. K., *J. Geophys. Res.*, 1992, **97**, 11789–11888.
15. Radha Krishna, M. and Mahadevan, T. M., Abstract volume Chapman conference on Stable Continental Region (SCR) earthquakes, 25–29 January, NGRI, Hyderabad, 1998, p. 42.
16. Kostrov, V. V., *Izv., Acad. Sci., USSR Phys. Solid Earth*, 1974, **1**, 23–44.
17. Brune, J. N., *J. Geophys. Res.*, 1968, **73**, 777–784.
18. Johnston, A. C., Report TR-102261, Electric Power Research Institute, 1993, chapter 3, pp. 3.1–3.59.
19. Veneziano, D., Report, Electric Power Research Institute, Palo Alto, California, 1984, vol. 58, p. 1768.
20. Jackson, J. and McKenzie, D., *Geophys. J.*, 1988, **93**, 45–73.
21. Gupta, H. K., *Tectonophysics*, 1985, **118**, 257–279.
22. Chadha, R. K. *et al.*, *Pure Appl. Geophys.*, 1997, **150**, 551–562.
23. Aki, K. and Richards, P., *Quantitative Seismology: Theory and Methods*, W. H. Freeman, San Fransisco, 1980.
24. Radhakrishna, B. P., *Curr. Sci.*, 1993, **64**, 787–793.
25. Widdowson, M., *Geol. Soc. Spl. Publ.*, 1997, **127**, 221–248.
26. De Mets, C., Gordon, R. G., Argus, F. and Stein, S., *Geophys. J. Int.*, 1990, **119**, 893–930.
27. Reddy, P. R., Kalachand Sain and Murty, A. S. N., *Curr. Sci.*, 1997, **73**, 796–800.
28. Rajendran, K. and Rajendran, C. P., *Tectonophysics*, 1999, **305**, 355–370.
29. Reddy, P. R., Mall, D. M. and Prasad, A. S. S. R. R. S., *Pure Appl. Geophys.*, 1997, **149**, 525–540.
30. Murrell, S. A. F., *Geol. Soc. London, Spl. Publ.*, 1986, **24**, 107–117.

ACKNOWLEDGEMENTS. We thank the anonymous reviewer for his very constructive suggestions. This work is part of a project funded by the Department of Science and Technology, Govt. of India, New Delhi. T.M.M. had the benefit of a brief interaction with Prof. A. C. Johnston during the last Chapman Conference held in NGRI, Hyderabad in January 1998.

Received 28 June 1999; revised accepted 6 January 2000